Re-thinking the role of motor cortex: Context-sensitive motor outputs?

Marta Gandolla,[a,*] Simona Ferrante,[a] Franco Molteni,[b] Eleonora Guanziroli,[b] Tiziano Frattini,[c] Alberto Martegani,[c] Giancarlo Ferrigno,[a] Karl Friston,[d] Alessandra Pedrocchi,[a,1] and Nick S. Ward[e,1]

[a]Politecnico di Milano, NearLab, Department of Electronics, Information and Bioengineering, Via G. Colombo 40, 20133 Milano, Italy

[b]Valduce Hospital, Villa Beretta Rehabilitation Center, Via N. Sauro 17, 23845 Costamasnaga, LC, Italy

[c]Valduce Hospital, Unità Operativa Complessa di Radiologia, via D. Alighieri 11, 22100 Como, Italy

[d]Wellcome Trust Centre for Neuroimaging, UCL Institute of Neurology, 12 Queen Square, London WC1N 3BG, UK

[e]Sobell Department of Movement Neuroscience, UCL Institute of Neurology, 33 Queen Square, London WC1N 3BG, UK

Marta Gandolla: marta.gandolla@polimi.it; Simona Ferrante: simona.ferrante@polimi.it; Franco Molteni: fmolteni@valduce.it; Eleonora Guanziroli: eleonora.guanziroli@gpop.it; Tiziano Frattini: tfrattini@valduce.it; Alberto Martegani: amartegani@valduce.it; Giancarlo Ferrigno: giancarlo.ferrigno@polimi.it; Karl Friston: k.friston@ucl.ac.uk; Alessandra Pedrocchi: alessandra.pedrocchi@polimi.it; Nick S. Ward: n.ward@ucl.ac.uk

*Corresponding author. Fax: + 39 0223999003. Email: marta.gandolla@polimi.it

[1]Pedrocchi Alessandra and Ward Nick S contributed equally to this work as joint last co-authors.

Accepted January 5, 2014.

Abstract

The standard account of motor control considers descending outputs from primary motor cortex (M1) as motor commands and efference copy. This account has been challenged recently by an alternative formulation in terms of active inference: M1 is considered as part of a sensorimotor hierarchy providing top–down proprioceptive predictions. The key difference between these accounts is that predictions are sensitive to the current proprioceptive context, whereas efference copy is not. Using functional electric stimulation to experimentally manipulate proprioception during voluntary movement in healthy human subjects, we assessed the evidence for context sensitive output from M1. Dynamic causal modeling of functional magnetic resonance imaging responses showed that FES altered proprioception increased the influence of M1 on primary somatosensory cortex (S1). These results disambiguate competing accounts of motor control, provide some insight into the synaptic mechanisms of sensory attenuation and may speak to potential mechanisms of action of FES in promoting motor learning in neurorehabilitation.

Abbreviations: ADF, ankle dorsiflexion; BA, Brodmann area; DCM, dynamic causal modeling; EPSP, excitatory postsynaptic potential; FES, functional electrical stimulation; FP, FES-induced ADF, while the subject remains relaxed; FV, FES-induced ADF concurrently with voluntary movement by the subject; fMRI, functional magnetic resonance imaging; M1, primary motor cortex; MNI, Montreal Neurological Institute; MRI, magnetic resonance imaging; P, passive dorsiflexion (by the experimenter) of the subject's

ankle; PR, parietal rostroventral area; ROI, region of interest; S1, primary somatosensory cortex; SII, secondary somatosensory cortex; V, voluntary ADF

Introduction

The execution of a voluntary movement requires the brain to integrate both the volitional intention to execute a given movement and knowledge about the state of the body (i.e. integrate sensory feedback). In humans, changing proprioceptive input influences motor cortex excitability (Léonard et al., 2013; Rosenkranz and Rothwell, 2012). Conversely, the response of somatosensory cortex neurons to proprioception is modified by the nature of the motor task (Chapman and Ageranioti-Bélanger, 1991; Cohen et al., 1994). Currently, motor control theory proposes that internal models generate motor commands that are sent to the periphery to produce the desired movement. In this account, internal models combine sensory inputs, prior knowledge and volitional intention to produce motor commands (Genewein and Braun, 2012). Forward models are thought to be responsible for predicting the sensory consequences of action, given the motor commands (Wolpert and Ghahramani, 2000; Wolpert and Kawato, 1998). It has been recently suggested that the updating of the internal model follows Bayesian principles (Genewein and Braun, 2012), combining a priori probability distributions and known levels of uncertainty of sensory feedback with sensorial consequences (Körding and Wolpert, 2004).

However, an alternative account of motor control has been proposed, drawing on the hierarchical generative models used in perceptual and active inference (Friston et al., 2009). In this account, motor cortex sends descending predictions of the sensory consequences of movement rather than the driving commands specified by optimal motor control. Here, proprioceptive prediction errors are generated at the level of the spinal cord and result in activation of motor neurons through classical reflex arcs. Although there are commonalities between the two accounts, the key difference is that under optimal control, given a same task and a same state of the system, motor signals are context-independent commands, whereas under active inference they are context-dependent predictions (Adams et al., 2012). In this study, we aim to disambiguate these accounts of motor control by experimentally manipulating both volitional movement and proprioception (i.e. context) and examining the effects on the interactions between cortical motor and sensory areas. In other words, we define an experimental protocol that only alters proprioception in different conditions while maintaining constant movement kinematics to reveal which areas and which connections are sensible to proprioception alteration. Our prediction was that modification of sensory feedback (reafference signals) during motor task execution will influence descending information from primary motor cortex (M1) — as predicted by the active inference account of motor control.

We used functional electrical stimulation (FES) to provide externally driven proprioceptive information during movement execution — in other words, to experimentally alter reafference. FES delivered to a mixed nerve trunk (i.e. nerve that contains both efferent motor and afferent sensory fibers) will synchronously depolarize motor and sensory axons that are bundled together, eliciting muscle contraction through two pathways. The first (direct descending pathway) conveys signals along the efferent motor fibers that generate muscle contraction by direct motoneuron depolarization. The second (indirect ascending pathway) communicates signals via the afferent sensory fibers (Collins, 2007) that code proprioceptive signals from muscle spindles, Golgi tendon organs and cutaneous receptors (Burke et al., 1983), but in particular Ia fibers responsible for muscle spindle information (Leis et al., 1995). This second pathway produces muscle contractions through a central mechanism, providing excitatory synaptic input to spinal neurons that recruit motor units in the natural order (Bergquist et al., 2011). Therefore, the proprioceptive signal elicited by the sensory fiber stimulation creates the impression that the muscle is

extended (i.e. muscle spindles discharge), and leads to firing of the motor neurons in order to produce a contraction. During FES, it has been demonstrated that this information can be useful at the level of the spinal cord, inducing a reinforcement of the muscle contraction through the myotatic reflex circuit, however few notions about altered proprioceptive information sent up to the cortex are available in the literature.

Our aim in this study was therefore to use FES during functional magnetic resonance imaging (fMRI) to investigate (i) where in the human brain altered proprioception information interacts with the intentional movement and (ii) how coupling or directed (effective) connectivity between these brain regions is influenced by altered proprioception. In particular, we were interested in the effect of altered proprioception on efferent signals from the primary motor cortex in order to disambiguate between two theoretical accounts of motor control.

Methods

Participants

Experiments were conducted with approval from the Villa Beretta Rehabilitation Centre ethics committee and all subjects gave informed written consent. Seventeen healthy volunteers (9 female, 8 male) with no neurological or orthopedic impairment were studied (mean age 36 ± 14 years, range 22–61).

Experimental set-up

The experimental set-up was comprised of a 1.5 T MRI scanner (GE Cv/I™), a motion capture system (Smart µg™; BTS) and an electrical stimulator (RehaStim proTM; HASOMED GmbH), as previously described and validated (Casellato et al., 2010; Gandolla et al., 2011).

fMRI task design

A 2 × 2 event-related fMRI design, with volitional intention [V: with the levels volitional and passive] and FES [F: with the levels present and absent] factors was performed using right ankle dorsiflexion (ADF). During a continuous 10 minute scanning session, subjects performed 20 alternate 9 s OFF and 21 s ON blocks. The 4 conditions that constituted our factorial design were performed during the ON blocks in a semi-randomized order: (i) FV = FES-induced ADF concurrently with voluntary movement by the subject; (ii) FP = FES-induced ADF, while the subject remains relaxed; (iii) V = voluntary ADF; (iv) P = passive dorsiflexion (by the experimenter) of the subject's ankle. The subjects were specifically instructed to remain completely relaxed during FP and P conditions and to equally voluntarily contribute during V and FV conditions. The dorsiflexions were paced every 3.5 s (for 6 repetitions) with an auditory cue. The auditory cues were presented through an earphone. Prior to scanning, subjects practiced the protocol until comfortable with the task; the experimenter was assisting the training to check the correct execution of the protocol. All subjects were free to choose the amplitude of their active movement to preclude fatigue. The experimenter moved the ankle to match to the movements during volitional dorsiflexion. Subjects were instructed to keep eyes closed and head movements were minimized with rubber pads and straps. To ensure minimum transmission of movements to the head, knees were bent with the subject's legs lying on a pillow.

FES stimulation paradigm

Functional electrical stimulation was applied to the peroneal nerve through superficial self-adhesive electrodes, with biphasic balanced current pulses at 20 Hz fixed frequency. The pulse width had a

trapezoidal profile (maximum pulse width 400 µs) and the current amplitude was set subject by subject so as to reproduce the same movement amplitudes as during voluntary movements, within the tolerance threshold. Current amplitude and pulse width were kept the same for both FP and FV conditions.

Data acquisition

A GE Cv/I system, operating at 1.5 T was used to acquire both T1-weigthed anatomical images (0.94 × 0.94 × 4 mm voxels) and T2*-weighted MRI transverse echo-planar images (1.8 × 1.8 × 4 mm voxels, TE = 50 ms) with blood oxygenation level dependent contrast. Each echoplanar image comprised 22 contiguous axial slices, positioned to cover the temporo-parietal and occipital lobes, with an effective repetition time of 3 s per volume. Due to technical reasons, it was not possible to acquire the cerebellum. The first six volumes were discarded to allow for T1 equilibration effects. A total of 200 brain volumes were acquired in a single run lasting 10 min.

Kinematic measures and analysis

3D trajectories of retro-reflective markers were acquired to measure the ankle angle during fMRI acquisitions and to determine the movement onset for event-related fMRI time series analysis. Two separate acquisition sessions were performed. The first was a static acquisition performed before the scanning, but while lying in the scanner, to estimate the coordinates of the medial and lateral malleoli for both lower limbs. During the static acquisition, a plate with 3 markers was placed on each tibia and 4 sticks with two markers each were placed on the four malleoli (Fig. 1, panel A). The relative positions of the malleoli with respect to the plates (i.e. left and right plates) were computed and the transformation matrices were estimated under the assumption that the tibia and malleoli were rigidly connected. The second acquisition, dynamic acquisition, was performed during the fMRI scanning. Only the two plates on the tibia were used to estimate the tibia 3D position and the malleoli. Four additional markers were placed over the four metacarpi (Fig. 1, panel B). In this configuration, markers were always visible during ADF for all different conditions. The sampling frequency was set at 120 Hz. The synchronization between the kinematic measures and the fMRI acquisitions was implemented using a further marker that was held by an operator in the cameras' field of view until the proper fMRI protocol started.

Marker trajectories were analyzed with a custom algorithm running in Matlab (Matlab R2010b). Trajectories from both static and dynamic acquisitions were interpolated with cubic splines to reconstruct the missing kinematic data for the few cases of marker obstruction and filtered with a second-order Butterworth low-pass filter (cut-off frequency = 1 Hz). For each leg, the ADF angle was calculated as follows: the mean points between the medial and lateral malleoli (mean malleolus) and between the medial and lateral metacarpi (mean metacarpus) were calculated. The ADF angle was taken as the angle between the line passing through the more proximal tibial marker and the mean malleolus and the line passing through the mean malleolus and the mean metacarpus. The automatic detection of onsets and amplitude measurements was checked carefully after algorithm identification.

fMRI data preprocessing

Imaging data were analyzed using Statistical Parametric Mapping (SPM8, Wellcome Department of Imaging Neuroscience, http://www.fil.ion.ucl.ac.uk/spm/) implemented in Matlab (Matlab R2010b). A skull stripping procedure – on the structural image for each subject – was performed to improve the coregistration of functional and structural images. All fMRI volumes were then realigned, and realignment parameters were assessed for excessive motion. A threshold of 4 mm in translation and 5° in rotation was applied (Johnstone et al., 2006). However, to suppress task related motion artifacts, realigned images were

also unwarped (Andersson et al., 2001). The skull stripped structural image was then coregistered to the mean image of the functional realigned volumes, and segmented. The spatial normalization transformation – to the Montreal Neurological Institute (MNI) reference brain in Talairach space (Talairach and Tournoux, 1988) – was then estimated using the segmented structural image. The structural image and functional volumes were normalized and resampled to 2 mm × 2 mm × 2 mm voxels. Functional normalized images were then smoothed with an isotropic 8 mm full-width half-maximum kernel (Friston et al., 1995). The time series in each voxel were high pass filtered at 1/128 Hz during subsequent modeling to remove low frequency confounds.

Statistical analysis

Statistical analysis was performed in two stages using the standard summary statistic approach. In the first stage, functional images were analyzed separately for each subject. From the kinematic measures, both the onset and the amplitude for each ankle dorsiflexion were extracted. Two ADF covariates were defined for each condition (i.e., FV, V, FP, P) — onsets and amplitude covariates. All ADF onsets belonging to the same condition were defined as a single event type and modeled as delta (stick) functions in the corresponding stimulus function. A second stimulus function for each condition (amplitude covariate) was defined as a delta function scaled by the actual amplitude of each ADF for each condition. The amplitude covariate was mean corrected and orthogonalized with respect to the correspondent onset covariate (Ward et al., 2008). All onset and amplitude stimulus functions were then convolved with a canonical hemodynamic response function, together with its temporal and dispersion derivatives (Ward et al., 2008) and used as regressors in a general linear model of the observed fMRI time series. Thus, for each subject, voxel-wise parameter estimates for each regressor were obtained. Linear contrasts of parameter estimates (reflecting mean effects and interactions) were generated for each subject (i.e. contrast images) and used for the creation of statistical parametric maps at the second (between subject) level.

Three contrasts of interest were tested: the main effect of FES, the main effect of voluntary movement and their interaction. The main effect of FES was defined as (FV + FP) − (P + V) and identifies regions that are activated during FES induced movements (i.e. FV, FP) over and above the non-FES induced movements (i.e. V, P). The main effect of voluntary movement was defined as (V + FV) − (P + FP) and identifies regions that are activated during a volitional movement (i.e. V, FV) over and above the non-voluntary movements (i.e. P, FP). The interaction was defined as (FV − V) − (FP − P) and identifies regions where the FES altered proprioception – in the context of volitional intent (i.e. FV − V) – produced a higher activation than FES altered proprioception in the absence of volitional movement (i.e. FP − P). Therefore, the interaction contrast represents the cortical representation of the proprioception "error" processing induced by FES, comparing its processing in the presence of movement/proprioception prediction (i.e., volitional context) or in its absence (i.e., passive context). Anatomical attribution was performed by carefully superimposing the maxima of significant effects both on the MNI brain and on the normalized structural images averaged across all subjects, and then labeling with the aid of the atlas of Duvernoy (1991).

Contrast images for each subject were entered into a one-sample t-test. Results were thresholded at $p < 0.05$ corrected for multiple comparisons within specific ROIs (i.e. small volume correction).

ROIs included contralateral M1 and S1. Other candidate regions included secondary somatosensory area SII, Brodmann area (BA) 7b and parietal rostroventral area (PR). Secondary somatosensory area (SII) has been selectively linked to proprioceptive processing and integration (Hinkley et al., 2007), attention to proprioceptive stimuli (Chen et al., 2010), painful and non-painful stimulus processing (Ferretti et al.,

2004) and complex object manipulation (Binkofski et al., 1999). BA7b and area PR have been identified as potential sites of sensorimotor integration (Hinkley et al., 2007) by virtue of their anatomical connections with premotor and primary motor cortices (Padberg et al., 2005).

Contralateral primary motor (M1) and primary sensory cortices (S1) were defined as 10 mm spheres centered respectively on [x = − 6, y = − 28, z = 60] and [x = − 4, y = − 46, z = 62] in the MNI coordinate system based on previous work (Freund et al., 2011). Bilateral secondary somatosensory cortices (SII) were defined as 10 mm spheres centered on [x = ± 58; y = − 27; z = 30] based on previous work (Ciccarelli et al., 2006; Iftime-Nielsen et al., 2012). PR and BA7b ROIs were defined as 10 mm spheres centered respectively on [x = ± 54; y = − 13; z = 19] and [x = ± 54; y = − 56; z = 23] in the MNI coordinate system again based on previous work (Hinkley et al., 2007).

Dynamic causal modeling (DCM) analysis

The functional images were smoothed with an isotropic 4 mm full-width maximum kernel for dynamic causal modeling (Friston et al., 2003) as implemented in SPM8 software (DCM10). A smaller smoothing kernel was used to ensure that ROIs from adjacent cortical areas did not overlap. The observed fMRI time series are used to estimate directed (effective) connectivity among regions or nodes (Friston et al., 2003), assuming that neuronal activity conforms to the following bilinear approximation:

$$\dot{x} = \left[A + \sum_{j=1}^{m} u_j B^j \right] * x + Cu.$$

Here, x represents the neuronal activity in a given ROI, and therefore this equation describes the evolution of neuronal activity in terms of a mixture of inputs from other areas and experimental input, u (this input corresponds exactly to the stimulus functions described under the general linear model above). The model parameters in the A matrix describe the average connectivity among brain regions during the experiment, irrespective of task modulation (endogenous connections). The model parameters of the B matrix represent the change in endogenous connections that can be elicited by an experimental variable (modulatory inputs). The model parameters in the C matrix represent the direct influences of an experimental variable on specific regions (driving inputs). Non-zero entries in the matrices [A, B, C] specify our assumptions about model structure. This model is supplemented with a forward model of how neuronal activity is transformed into the measured fMRI response (Friston et al., 2003). Estimated connectivity parameters describe the direction and strength of connectivity among brain regions. In addition to providing Bayesian estimates of the model parameters, model inversion provides an approximation to model evidence. This free energy approximation can be used to identify the model that is most likely given the observed data, using Bayesian model selection (Penny et al., 2004).

The anatomical nodes of our DCM were derived from the interaction contrast, (FV − V) − (FP − P) from the general linear model (standard SPM) analysis, and therefore will be described in the results session (DCM results section). The general linear model was reformulated to specify the driving and modulatory experimental inputs. These comprised a stimulus function representing the effect of descending voluntary signals — V (onsets from V and FV conditions; i.e. u_1); a second input encoding the contribution of ascending functional electrical stimulation to proprioceptive input — E (onsets from FV and FP conditions; i.e. u_2) and a third input representing underlying proprioceptive input from all movements — P

(onsets from all conditions; i.e. u_3). To summarize the regional activity of each subject, an F-contrast was performed across all covariates of the new design matrix for each subject. Functionally, the choice of subject-specific coordinates was informed by the location of the group maxima, in that we selected subject-specific maxima in regions that were within 5 mm of the group maxima and within the same gyrus. For each subject, regional responses were summarized with the first eigenvariate of a sphere (4 mm diameter) centered in the subject-specific maxima. Crucially, we allowed E (altered proprioception) to modulate different connections or combination of connections — where modulation of self-connections corresponds to a modulation of intrinsic excitability. The rationale for modeling the modulatory effects of E is that we wanted to examine both the driving effects of stimulation and activity-dependent effects on cortical excitability or gain.

We assessed the evidence for competing models or hypotheses using Bayesian model selection. The optimal model – with the highest evidence – represents the best balance between model fit and complexity with respect to the others. Model comparison and selection rest on the model evidence, in other words, the probability of observing experimentally measured BOLD signals under a particular DCM. Model selection at the group level was based on fixed effects inference, under the assumption that the underlying functional architecture is conserved over (our healthy) subjects. The ensuing posterior probability of each model reflects the evidence for one model, relative to the others (Stephan et al., 2010).

Results

Kinematic measures

Mean values along with their standard deviations for the dorsiflexion angles for each condition across all blocks calculated over 30 samples (6 ADF/block, 5 blocks per condition) resulted to be as follows. Mean amplitude across subjects along with its standard deviation for V condition was $37° \pm 5°$, for FV condition $35° \pm 6°$, for FP condition $26° \pm 5°$, and for P condition $32° \pm 5°$.

Group fMRI effects

Realignment parameters were assessed for excessive motion, and only one subject violated our criteria (see Inline Supplementary Table S1). This subject was therefore discarded from the group analysis. Without this single subject, the maximum translational displacement was 3.282 mm in all directions and the maximum rotational displacement was $0.061°$. All four conditions show clear activation in motor and somatosensory areas known to be involved in ADF execution and in accord with previous studies (Ciccarelli et al., 2005; Dobkin et al., 2004; Iftime-Nielsen et al., 2012), as expected (Fig. 2, Tables 1 and 2).

Inline Supplementary Table S1

Inline Supplementary Table S1

Realignment parameters were assessed for excessive motion, and only one subject violated our criteria (see Inline Supplementary Table S1). This subject was therefore discarded from the group analysis. Without this single subject, the maximum translational displacement was 3.282 mm in all directions and the maximum rotational displacement was $0.061°$. All four conditions show clear activation in motor and somatosensory areas known to be involved in ADF execution and in accord with previous studies

(Ciccarelli et al., 2005; Dobkin et al., 2004; Iftime-Nielsen et al., 2012), as expected (Fig. 2, Tables 1 and 2).

Inline Supplementary Table S1 can be found online at http://dx.doi.org/10.1016/j.neuroimage.2014.01.011.

A positive interaction ([FV − V] > [FP − P]) was seen in both M1 and S1. In other words, the effect of altered proprioception depends on volitional movement in both M1 and S1 (Fig. 3). To understand how these interactions were generated – in terms of driving and modulatory inputs to M1 and S1 – we now turn to the results of dynamic causal modeling (DCM).

DCM results

Given the results for the interaction above, we defined a basic fully connected two area DCM (Fig. 4), with M1 and S1 as the selected nodes (i.e. x_1 = M1; x_2 = S1). The coordinates of the ROIs were consistent across subjects (see Inline Supplementary Table S2). The average coordinates, along with their variability in terms of standard deviation (±) were as follows. For M1 area x = − 2 ± 1.75; y = − 26 ± 3.01; z = 62 ± 2.91, whereas for S1 area x = − 7 ± 2.62; y = − 44 ± 2.37; z = 66 ± 1.86.

> **Inline Supplementary Table S2**
>
> Inline Supplementary Table S2

Given the results for the interaction above, we defined a basic fully connected two area DCM (Fig. 4), with M1 and S1 as the selected nodes (i.e. x_1 = M1; x_2 = S1). The coordinates of the ROIs were consistent across subjects (see Inline Supplementary Table S2). The average coordinates, along with their variability in terms of standard deviation (±) were as follows. For M1 area x = − 2 ± 1.75; y = − 26 ± 3.01; z = 62 ± 2.91, whereas for S1 area x = − 7 ± 2.62; y = − 44 ± 2.37; z = 66 ± 1.86.

Inline Supplementary Table S2 can be found online at http://dx.doi.org/10.1016/j.neuroimage.2014.01.011.

The effects of experimental inputs (i.e. *C* matrix) were based upon prior knowledge about functional anatomy: V was assumed to drive M1, modeling top–down intentional signals during voluntary movements from pre-motor and supplementary motor cortices (i.e. C_{11} = 1); indeed, we know that premotor areas project to M1 supragranular layers (Donoghue and Parham, 1983). P was assumed to drive S1 (i.e. C_{23} = 1), modeling the proprioceptive and somatosensory consequences of movement (e.g. ascending afferents from muscle spindles and Golgi tendon) that are known to convey information to sensory areas (Schwarz et al., 1973); E was specified as driving S1 as well (i.e. C_{22} = 1), modeling the further sensory contribution due to electrical stimulation (Fig. 4). Since E was allowed to modulate all possible combinations of connections, the base model produced 15 variants, allowing for all endogenous connections (including self-connections) and their combinations to be modulated by the E (i.e. all different possible combinations of the B_1 matrix). Since we only had 15 models, we didn't perform any family grouping, and we directly performed Bayesian model selection among our model space.

The winning model (Fig. 5 — panel A) suggests that E exerts a modulatory effect on the reciprocal connections between M1 and S1 and S1 self-connection. This winning model showed a large difference in log evidence, with respect to the next best model; with strong evidence in its favor — following the Bayes factor interpretation (Penny et al., 2004). The lower panel of Fig. 5 (Fig. 5 — panel B) shows the profile of log evidence (over the 15 models) and the ensuing posterior probabilities. In particular, the posterior

probability of this winning model over alternative models was 0.97. In other words, assuming uniform priors over the 15 models, we can be 97% certain that the model in Fig. 5 is the most likely model.

In terms of endogenous (A) connectivity (Fig. 5, blue numbers), it can be seen that M1 and S1 self-connections have negative values reflecting the self-inhibition required for system stability (− 0.67 and − 0.46, respectively). In contrast, the reciprocal connections between the M1 and S1 have positive values (reflecting an excitatory influence). In particular, the M1 to S1 connection is 0.11 and S1 to M1 is 0.51. This means that the connection from the sensory to motor cortex is about five times stronger than the reciprocal connection. When considering the driving inputs (Fig. 5, green numbers), top–down volitional discharge (V) to M1 has a positive value: 0.28. Proprioception (P) discharge to S1 has a high impact on the system (0.6) and it is further increased by the effect of stimulation (E) by about 15%.

The modulatory effect of altered proprioceptive input (Fig. 5, red numbers) indicates which connections are modulated by E in the winning model; i.e., context-dependent changes in connectivity. The modulatory effects indicate that the increase in the sensitivity of recurrent inhibition in S1 is quite marked (37%). M1 self-connection is not directly modulated by E. Moreover, this model suggests an impressive increase of the influence of M1 on S1 with a 181% increase in the sensitivity of S1 to M1 afferents. In addition, there is an increase in S1 to M1 connection; namely, the outgoing signals from S1 have a greater influence (25%) over M1 during concurrent functional electrical stimulation. In summary, the most prescient influence of electrical stimulation was to massively and selectively increase the sensitivity of S1 populations to projections from M1.

Discussion

The aim of the present study was to examine the neuronal substrate of the interaction between voluntary movement execution and sensory feedback. In particular, we hoped to discriminate between different accounts of motor control; i.e., descending signals from M1 as driving motor commands (the optimal control account) or as predictions of desired proprioceptive consequences (the active inference account). FES was used to alter proprioception during movement execution. Our results demonstrated that (i) the interaction between volitional intention and sensory feedback occurs predominantly in primary cortical areas (i.e. M1, S1); (ii) the altered effect of proprioception during concurrent movement can be explained by an increase in the influence of M1 on S1 (as well as S1 self-connections, with less effect on S1 to M1 connections); (iii) the efferent information from M1 (analogous to corollary discharge from M1 to S1) is modified by artificial modified proprioception and is therefore more likely to represent context-dependent backward projections conveying proprioception predictions.

Sensorimotor integration can be seen in terms of input–output systems, where – in our case – input is (ascending) sensory feedback or (descending) cognitive or predictive processes and output is (descending) information sent to the periphery or (ascending) to high levels of the sensorimotor hierarchy. Our (general linear model) results suggest an effect of additional (ascending) proprioceptive input during FES in M1 and S1, but not in any other brain regions. Others have shown reduced activation in SII for active compared to passive movement during stimulation (i.e. FV compared to FP in our study), suggesting that SII might be involved in the matching of an internal model with the sensory input (Iftime-Nielsen et al., 2012). However, in our study SII activity was greater in the stimulation conditions compared to no stimulation, suggesting that SII is the recipient of the FES stimuli and does not reflect integration of sensory signals with motor commands (Christensen and Grey, 2013; Francis et al., 2009). Our subjects were naïve to FES and SII activation may simply reflect increased attention to proprioceptive stimuli (Chen et al., 2010; Hinkley et al., 2007) in both stimulation conditions. The parietal rostroventral (PR) area

showed an activation pattern similar to SII, and so might have a similar role in processing proprioception coupled with movement execution, as suggested in the literature (Hinkley et al., 2007). In addition to proprioception processing, the role of SII and PR areas during stimulation conditions (i.e. FV, FP) might be linked to cutaneous afferent input (i.e., somatosensory processing), but this does not appear to be modulated by the presence or absence of volitional intention. Previous work suggests that SII remains significantly active in the case of electrical stimulation with low current values, which is likely to exclusively stimulate the cutaneous afferent fibers mediating cutaneous receptor input (Backes et al., 2000).

The precuneus was activated in all conditions suggesting that it is a recipient and processor of proprioception stimuli, but not selectively involved in sensorimotor interaction. Despite its proposed role as a sensorimotor integration center, BA7b was not active in any condition. This is similar to findings of Hinkley et al. (2007) who did not find any consistent BA7b activation during tactile stimulation with hand movement.

We investigated the neuronal interactions that may underlie sensorimotor integration with DCM (Friston et al., 2003), which served to assess the relative plausibility of alternative neurophysiological explanations for the effects we established using conventional analyses (Stephan and Roebroeck, 2012). DCM provided plausible results for intrinsic connectivity: the presence of the positive (descending) input to M1 is likely to represent projections from higher order areas, including premotor areas and supplementary motor area (Picard and Strick, 2001). Given that M1 and S1 are reciprocally connected, especially via cortical layers V and VI (Rocco and Brumberg, 2007), updating of motor plans (or predictions) should be mediated by sensory areas, which is reflected in the excitatory S1 to M1 connection. S1 activity is dominated by the external inputs: S1 granular layer receives ascending inputs from spinal circuits, typically through the thalamic pathway (Padberg et al., 2005) and specifically, part of the primary somatosensory cortex, Brodmann area 3a, receives substantial input from muscle proprioceptors (Körding and Wolpert, 2004). This is reflected in the positive inputs to S1. Our main aim was to examine how this directed connectivity was modulated by proprioception alteration. We observed two effects of proprioceptive alteration: (i) an increase in S1 self-inhibition, indicating a decrease in sensitivity to non-specific afferents and (ii) a large increase in the facilitatory effect of M1 on S1, reflecting a large and selective increase in the gain of S1 to M1 afferents. The increase of influence of S1 on M1 was by contrast small, probably because the proprioceptive inputs are passed from S1 to M1 — independently of the actual performance of the movement (i.e. they are context-independent). Crucially, the fact that altered proprioception selectively increased input to S1 from M1 suggests that the effect of stimulation depends upon the presence of top–down volitional or intentional signals. This is because the primary determinant of M1 activity is an effect of volitional movement. In this context, one can regard the modulation of the M1 to S1 connection as mediating the interaction between altered proprioception and volitional movement (as encoded by the activity of M1).

It is interesting to consider these results under alternative accounts of motor control. Classical accounts based upon optimal control theory suggest that M1 is responsible for generating the descending motor commands to produce a desired trajectory (Wolpert and Kawato, 1998). Active inference, on the other hand, suggests that M1 sends predictions of the sensory consequences of a movement to the periphery (Friston et al., 2009). Therefore, the information sent from M1 to S1 (and from M1 to the periphery) should be different under the two accounts. Proprioceptive prediction has a "sensorial" nature, whereas motor commands are signals that drive muscles. Crucially, the connection from M1 to the periphery (and to S1) should be a context-independent driving connection in the case of optimal motor control accounts,

and conversely a context-dependent descending prediction in the case of active inference. The motor command (optimal control) needed to perform ankle dorsiflexion should have the same influence on S1 regardless of any altered proprioception, since the motor output is the same in all conditions, and the motor command to execute the task is context-independent, under the hypothesis that the subjects equally voluntarily contributed during FV and V conditions. On the other hand, proprioception predictions (under active inference) should be modified according to proprioceptive state (i.e. it depends on whether FES is present or not). The DCM results are more consistent with the active inference account — since we observed a massive modulatory effect on the M1 to S1 connection, suggesting that the influence of M1 on S1 is context-sensitive.

A context-sensitive or modulatory aspect of descending signals from M1 is consistent with the observation that there spinal targets — spinal interneurons, Renshaw cells and motor neurons — express NMDA receptors have non-linear and modulatory properties (Adams et al., 2012). Furthermore, if the descending connections from M1 are indeed modulatory, they should have smaller excitatory postsynaptic potentials (EPSPs) and exhibit non-linear characteristics. Indeed, EPSPs from single cortico-spinal fibers are smaller in magnitude than correspondent single fiber cortico-cortical EPSPs (Andersen et al., 1990). In the optimal control account, output from M1 is thought of as 'efference copy' to S1 or the cerebellum (Blakemore et al., 2001). However, efference copy is – by definition – simply a copy of motor commands and does not depend upon proprioceptive context. The fact that we have demonstrated a context-sensitive influence of M1 speaks against the notion of 'efference copy' and more in favor of M1 generating 'corollary discharge' — in the sense of predicting the sensory consequences of action.

We suggest that the differential effect of proprioception during concurrent voluntary movement in healthy subjects enhances the influence of M1 on S1, thereby amplifying the gain of the somatosensory predictions (corollary discharge) to S1. There was no behavioral consequence of this context specific alteration in M1 output. This is however in line with the hypothesis that spinal circuits fulfill proprioceptive predictions (Adams et al., 2012). In other words, if altered proprioceptive feedback (from FES) matches the altered proprioceptive prediction (from M1), prediction error will not change and so motor output to the muscles driven by reflex arcs will not change.

Our study also validates the use of FES as a tool to improve motor function after central nervous system injury. TMS studies show that FES-induced repetitive movements enhance motor cortex excitability and facilitate motor-evoked potentials of the tibialis anterior (Knash et al., 2003), especially in the context of ambulation (Kido Thompson and Stein, 2004) and concurrent voluntary activation (Barsi et al., 2008) — presenting long-lasting facilitatory effects that are focally modulated by a voluntary cortical drive (Khaslavskaia and Sinkjaer, 2005). Stimulation of the common peroneal nerve paired with TMS, applied during swing phase of gait-induced bidirectional changes in cortico-motor excitability, consistent with the Hebbian principle of activity-dependent neuroplasticity (Stinear and Hornby, 2005). FES seems to be particularly effective when augmenting attempted volitional movement, although the mechanism is not yet clear. On the basis of our results, we hypothesize that FES interacts with attempted volitional movement to produce long lasting motor improvement (in dorsiflexion) by increasing the influence of M1 on S1.

An important limitation of this study was the inability to collect data from the cerebellum due to technical constraints. We tried to overcome this limitation as far as we could, by training the subjects outside the scanner so that they were familiar with the stimulus during FES conditions. However, the cerebellum is thought to be part of the motor control loop, and it has been shown to be differentially involved during voluntary and non-voluntary FES (Iftime-Nielsen et al., 2012). Moreover, computing predictions of sensor consequences is seen in literature as a major role of the cerebellum (together with the parietal cortex)

within the sensory-motor control loop ([Blakemore et al., 2001](#)). The cerebellum is anatomically connected with S1 and M1 (with afferent and efferent pathways) and we would expect to see a modulatory activity in the cerebellum as well, that could enrich our model. Further studies are recommended to explore this aspect.

We measured the executed movement during scanning to control for movement parameters across sessions. We set movement rate at 0.3 Hz ([Ciccarelli et al., 2005](#)), and the amplitude was determined by the subject, as an egocentric reference task: this led to a broad range of amplitudes (10°–71°). However, [Ciccarelli et al. (2005)](#) did not find any effect of movement amplitude (10°–55°), suggesting that if the movement is egocentric and self-paced, there is no difference in associated cortical activity. Having said this, movement amplitude was included as covariate in our analysis, to ensure our analyses were robust to possible differences across subjects, specifically due to this parameter.

Conclusions

In conclusion, our study has highlighted that M1 and S1 exhibit a profound interaction between artificially altered sensory feedback and volitional movement. Changes in coupling between these regions support an active inference account of motor control, in which sensorimotor integration rests upon the context-sensitive assimilation of descending motor predictions. The implicit functional architecture may be important for future studies in healthy aging individuals or patients (e.g. stroke) or indeed during rehabilitation.

Acknowledgments

Conflict of interest

There are no conflicts of interest for any author.

References

Adams R.A., Shipp S., Friston K.J. Predictions not commands: active inference in the motor system. Brain Struct. Funct. 2012 [PMCID: PMC3637647]

Andersen P., Raastad M., Storm J.F. Excitatory synaptic integration in hippocampal pyramids and dentate granule cells. Cold Spring Harb. Symp. Quant. Biol. 1990;55:81–86. [PubMed: 2132857]

Andersson J.L., Hutton C., Ashburner J., Turner R., Friston K.J. Modeling geometric deformations in EPI time series. NeuroImage. 2001;13:903–919. [PubMed: 11304086]

Backes W.H., Mess W.H., van Kranen-Mastenbroek V., Reulen J.P.H. Somatosensory cortex responses to median nerve stimulation: fMRI effects of current amplitude and selective attention. Clin. Neurophysiol. 2000;111:1738–1744. [PubMed: 11018487]

Barsi G.I., Popovic D.B., Tarkka I.M., Sinkjaer T., Grey M.J. Cortical excitability changes following grasping exercise augmented with electrical stimulation. Exp. Brain Res. 2008;191:57–66. [PubMed: 18663439]

Bergquist A.J., Clair J.M., Lagerquist O., Mang C.S., Okuma Y., Collins D.F. Neuromuscular electrical

stimulation: implications of the electrically evoked sensory volley. Eur. J. Appl. Physiol. 2011;111:2409–2426. [PubMed: 21805156]

Binkofski F., Buccino G., Posse S., Seitz R.J., Rizzolatti G., Freund H. A fronto-parietal circuit for object manipulation in man: evidence from an fMRI-study. Eur. J. Neurosci. 1999;11:3276–3286. [PubMed: 10510191]

Blakemore S.J., Frith C.D., Wolpert D.M. The cerebellum is involved in predicting the sensory consequences of action. Neuroreport. 2001;12:1879–1884. [PubMed: 11435916]

Burke D., Gandevia S.C., McKeon B. The afferent volleys responsible for spinal proprioceptive reflexes in man. J. Physiol. 1983;339:535–552. [PubMed: 6887033]

Casellato C., Ferrante S., Gandolla M., Volonterio N., Ferrigno G., Baselli G., Frattini T., Martegani A., Molteni F., Pedrocchi A. Simultaneous measurements of kinematics and fMRI: compatibility assessment and case report on recovery evaluation of one stroke patient. J. Neuroeng. Rehabil. 2010;7:49. [PubMed: 20863391]

Chapman C.E., Ageranioti-Bélanger S.A. Discharge properties of neurones in the hand area of primary somatosensory cortex in monkeys in relation to the performance of an active tactile discrimination task. I. Areas 3b and 1. Exp. Brain Res. 1991;87:319–339. [PubMed: 1769386]

Chen T.L., Babiloni C., Ferretti A., Perrucci M.G., Romani G.L., Rossini P.M., Tartaro A., Del Gratta C. Effects of somatosensory stimulation and attention on human somatosensory cortex: an fMRI study. NeuroImage. 2010;53:181–188. [PubMed: 20598908]

Christensen M.S., Grey M.J. Modulation of proprioceptive feedback during functional electrical stimulation: an fMRI study. Eur. J. Neurosci. 2013;37:1766–1778. [PubMed: 23461704]

Ciccarelli O., Toosy A.T., Marsden J.F., Wheeler-Kingshott C.M., Sahyoun C., Matthews P.M., Miller D.H., Thompson A.J. Identifying brain regions for integrative sensorimotor processing with ankle movements. Exp. Brain Res. 2005;166:31–42. [PubMed: 16034570]

Ciccarelli O., Toosy A.T., Marsden J.F., Wheeler-Kingshott C.M., Miller D.H., Matthews P.M., Thompson A.J. Functional response to active and passive ankle movements with clinical correlations in patients with primary progressive multiple sclerosis. J. Neurol. 2006;253:882–891. [PubMed: 16619123]

Cohen D.A., Prud'homme M.J., Kalaska J.F. Tactile activity in primate primary somatosensory cortex during active arm movements: correlation with receptive field properties. J. Neurophysiol. 1994;71:161–172. [PubMed: 8158225]

Collins D.F. Central contributions to contractions evoked by tetanic neuromuscular electrical stimulation. Exerc. Sport Sci. Rev. 2007;35:102–109. [PubMed: 17620928]

Dobkin B.H., Firestine A., West M., Saremi K., Woods R. Ankle dorsiflexion as an fMRI paradigm to assay motor control for walking during rehabilitation. NeuroImage. 2004;23:370–381. [PubMed: 15325385]

Donoghue J.P., Parham C. Afferent connections of the lateral agranular field of the rat motor cortex. J. Comp. Neurol. 1983;217:390–404. [PubMed: 6886060]

Duvernoy H.M. Springer-Verlag; New York, USA: 1991. The Human Brain: Surface, Blood Supply, and Three-dimensional Anatomy.

Ferretti A., Del Gratta C., Babiloni C., Caulo M., Arienzo D., Tartaro A., Rossini P.M., Romani G.L. Functional topography of the secondary somatosensory cortex for nonpainful and painful stimulation of median and tibial nerve: an fMRI study. NeuroImage. 2004;23:1217–1225. [PubMed: 15528121]

Francis S., Lin X., Aboushoushah S., White T.P., Phillips M., Bowtell R., Constantinescu C.S. fMRI analysis of active, passive and electrically stimulated ankle dorsiflexion. NeuroImage. 2009;44:469–479. [PubMed: 18950717]

Freund P., Weiskopf N., Ward N.S., Hutton C., Gall A., Ciccarelli O., Craggs M., Friston K., Thompson A.J. Disability, atrophy and cortical reorganization following spinal cord injury. Brain. 2011;134:1610–1622. [PubMed: 21586596]

Friston K.J., Ashburner J., Frith C.D., Poline J.B., Heather J.D., Frackowiak R.S.J. Spatial registration and normalization of images. Hum. Brain Mapp. 1995;3:165–189.

Friston K.J., Harrison L., Penny W. Dynamic causal modelling. NeuroImage. 2003;19:1273–1302. [PubMed: 12948688]

Friston K.J., Daunizeau J., Kiebel S.J. Reinforcement learning or active inference? PLoS ONE. 2009;4:e6421. [PubMed: 19641614]

Gandolla M., Ferrante S., Casellato C., Ferrigno G., Molteni F., Martegani A., Frattini T., Pedrocchi A. fMRI brain mapping during motion capture and FES induced motor tasks: signal to noise ratio assessment. Med. Eng. Phys. 2011;33:1027–1032. [PubMed: 21550290]

Genewein T., Braun D.A. A sensorimotor paradigm for Bayesian model selection. Front. Hum. Neurosci. 2012;6:291. [PubMed: 23125827]

Hinkley L.B., Krubitzer L.A., Nagarajan S.S., Disbrow E.A. Sensorimotor integration in S2, PV, and parietal rostroventral areas of the human sylvian fissure. J. Neurophysiol. 2007;97:1288–1297. [PubMed: 17122318]

Iftime-Nielsen S.D., Christensen M.S., Vingborg R.J., Sinkjaer T., Roepstorff A., Grey M.J. Interaction of electrical stimulation and voluntary hand movement in SII and the cerebellum during simulated therapeutic functional electrical stimulation in healthy adults. Hum. Brain Mapp. 2012;33:40–49. [PubMed: 21591025]

Johnstone T., Ores Walsh K.S., Greischar L.L., Alexander A.L., Fox A.S., Davidson R.J., Oakes T.R. Motion correction and the use of motion covariates in multiple-subject fMRI analysis. Hum. Brain Mapp. 2006;27:779–788. [PubMed: 16456818]

Khaslavskaia S., Sinkjaer T. Motor cortex excitability following repetitive electrical stimulation of the common peroneal nerve depends on the voluntary drive. Exp. Brain Res. 2005;162:497–502. [PubMed: 15702321]

Kido Thompson A., Stein R.B. Short-term effects of functional electrical stimulation on motor-evoked potentials in ankle flexor and extensor muscles. Exp. Brain Res. 2004;159:491–500. [PubMed: 15243732]

Knash M.E., Kido A., Gorassini M., Chan K.M., Stein R.B. Electrical stimulation of the human common peroneal nerve elicits lasting facilitation of cortical motor-evoked potentials. Exp. Brain Res. 2003;153:366–377. [PubMed: 14610631]

Körding K.P., Wolpert D.M. Bayesian integration in sensorimotor learning. Nature. 2004;427:244–247. [PubMed: 14724638]

Leis A.A., Grubwieser G.J., Schild J.H., West M.S., Stokic D.S. Control of Ia afferent input to Triceos Surae (Soleus) locomotor nucleus precedes agonist muscle activation during gait. J. Electromyogr. Kinesiol. 1995;5:95–100. [PubMed: 20719640]

Léonard G., Mercier C., Tremblay L.E. Effect of repetitive afferent electrical stimulation of the lower limb on corticomotor excitability and implications for rehabilitation. J. Clin. Neurosci. 2013;20:435–439. [PubMed: 23228660]

Padberg J., Disbrow E., Krubitzer L. The organization and connections of anterior and posterior parietal cortex in titi monkeys: do new world monkeys have an area 2? Cereb. Cortex. 2005;15:1938–1963. [PubMed: 15758196]

Penny W.D., Stephan K.E., Mechelli A., Friston K.J. Comparing dynamic causal models. NeuroImage. 2004;22:1157–1172. [PubMed: 15219588]

Picard N., Strick P.L. Imaging the premotor areas. Curr. Opin. Neurol. 2001;11:663–672.

Rocco M.M., Brumberg J.C. The sensorimotor slice. J. Neurosci. Methods. 2007;162:139–147. [PubMed: 17307257]

Rosenkranz K., Rothwell J.C. Modulation of proprioceptive integration in the motor cortex shapes human motor learning. J. Neurosci. 2012;32:9000–9006. [PubMed: 22745499]

Schwarz D.W., Deecke L., Fredrickson J.M. Cortical projection of group I muscle afferents to areas 2, 3a, and the vestibular field in the rhesus monkey. Exp. Brain Res. 1973;17:516–526. [PubMed: 4200363]

Stephan K.E., Roebroeck A. A short history of causal modeling of fMRI data. NeuroImage. 2012;62:856–863. [PubMed: 22248576]

Stephan K.E., Penny W.D., Moran R.J., den Ouden H.E., Daunizeau J., Friston K.J. Ten simple rules for dynamic causal modeling. NeuroImage. 2010;49:3099–3109. [PubMed: 19914382]

Stinear J.W., Hornby T.G. Stimulation-induced changes in lower limb corticomotor excitability during treadmill walking in humans. J. Physiol. Lond. 2005;567:701–711. [PubMed: 15975980]

Talairach J., Tournoux P. Thieme; Stuttgart: 1988. Co-planar Stereotaxic Atlas of the Human Brain.

Ward N.S., Swayne O.B.C., Newton J.M. Age-dependent changes in the neural correlates of force modulation: an fMRI study. Neurobiol. Aging. 2008;29:1434–1446. [PubMed: 17566608]

Wolpert D.M., Ghahramani Z. Computational principles of movement neuroscience. Nat. Neurosci. Suppl. 2000;3:1212–1217.

Wolpert D.M., Kawato M. Multiple paired forward and inverse models for motor control. Neural Netw. 1998;11:1317–1329. [PubMed: 12662752]

Figures and Tables

Table S1

Realignment parameters.

Maximum of the absolute value of the realignment parameters in each translational and rotational direction.

Subject	Translation [mm]			Rotation [°]		
	x	y	z	pitch	roll	yaw
1	0.404	0.558	2.492	0.036	0.011	0.013
2	10.130	1.172	1.972	0.023	0.031	0.131
3	0.330	0.189	0.860	0.018	0.003	0.007
4	0.408	0.332	1.044	0.020	0.007	0.004
5	0.575	0.291	2.078	0.021	0.023	0.021
6	0.929	0.150	0.624	0.016	0.003	0.014
7	0.248	0.806	2.057	0.023	0.003	0.007
8	1.581	0.194	1.669	0.031	0.016	0.023
9	0.368	0.388	0.943	0.015	0.009	0.008
10	0.121	0.575	1.054	0.061	0.004	0.003
11	0.391	0.188	0.808	0.006	0.008	0.005
12	2.754	0.491	3.088	0.026	0.030	0.038
13	0.306	0.196	1.718	0.012	0.013	0.006
14	1.787	0.423	3.282	0.030	0.023	0.028
15	0.329	0.416	1.931	0.032	0.004	0.005
16	0.390	0.322	1.562	0.010	0.008	0.007
17	0.301	0.216	1.089	0.011	0.006	0.005

Table S2

Coordinates for DCM regions of interest in the MNI space.

Subject	M1			S1		
	x [mm]	y [mm]	z [mm]	x [mm]	y [mm]	z [mm]
1	-2	-22	62	-4	-42	64
3	-2	-26	64	-4	-42	62
4	-6	-28	66	-8	-48	68
5	-2	-22	62	-4	-48	68
6	-2	-30	64	-4	-42	66
7	-2	-22	58	-8	-46	66
8	-4	-28	64	-8	-44	68
9	-2	-30	62	-10	-46	64
10	0	-22	62	-4	-42	64
11	-4	-26	56	-10	-44	66
12	-6	-26	60	-8	-46	68
13	-2	-24	56	-8	-42	66
14	-4	-28	64	-4	-48	68

|						
15	-2	-24	64	-10	-46	64
16	0	-28	62	-4	-42	66
17	-2	-30	62	-10	-44	66

Fig. 1
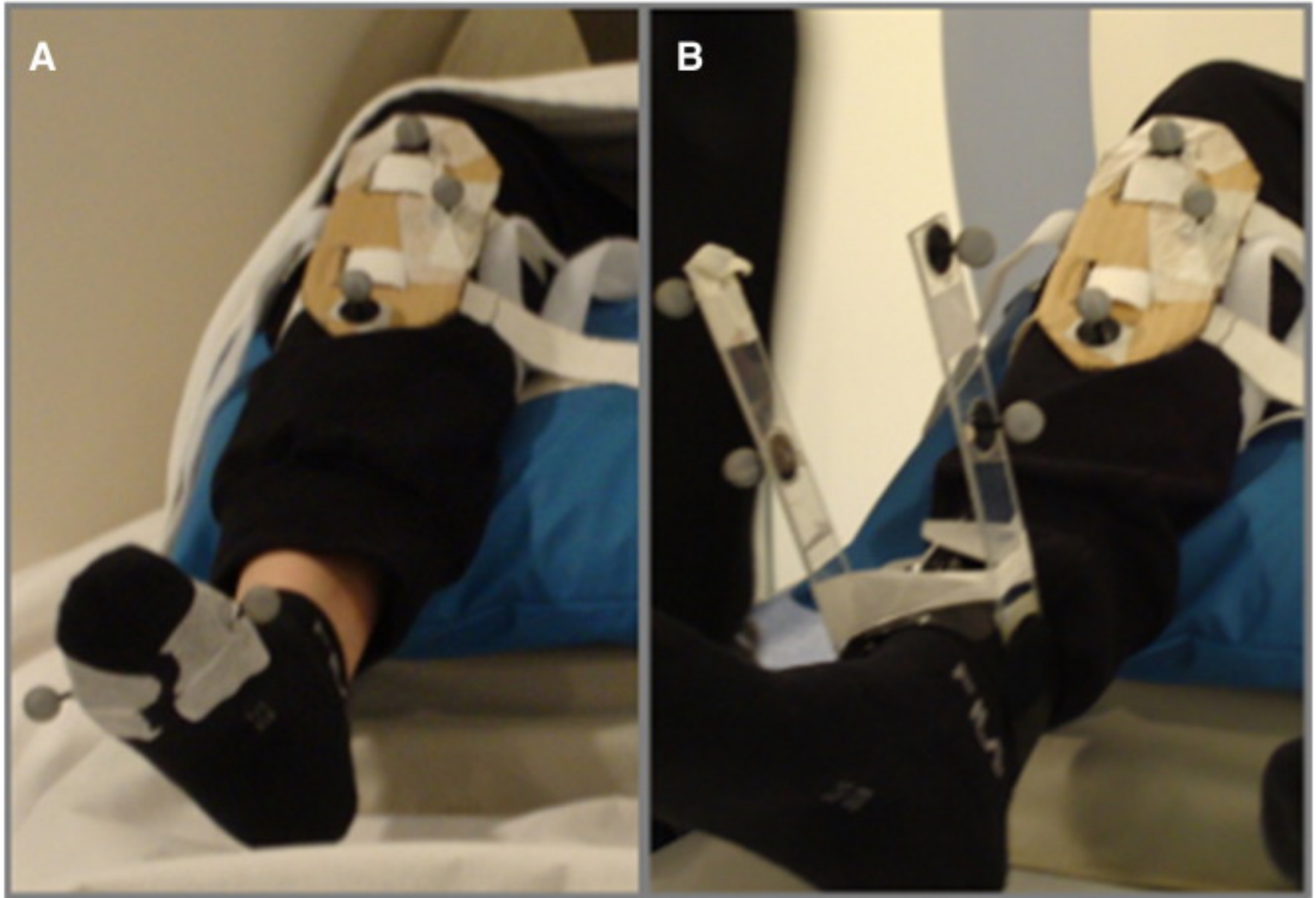
Markers disposition. (A) Static acquisition: position of the 7 markers for each leg. Markers were placed on each tibia and 4 sticks with two markers each were placed on the four malleoli. (B) Dynamic acquisition: disposition of the 5 markers for each leg. The markers on the tibias were left in the same position as (A), 4 markers were placed on the 4 metacarpi.

Fig. 2
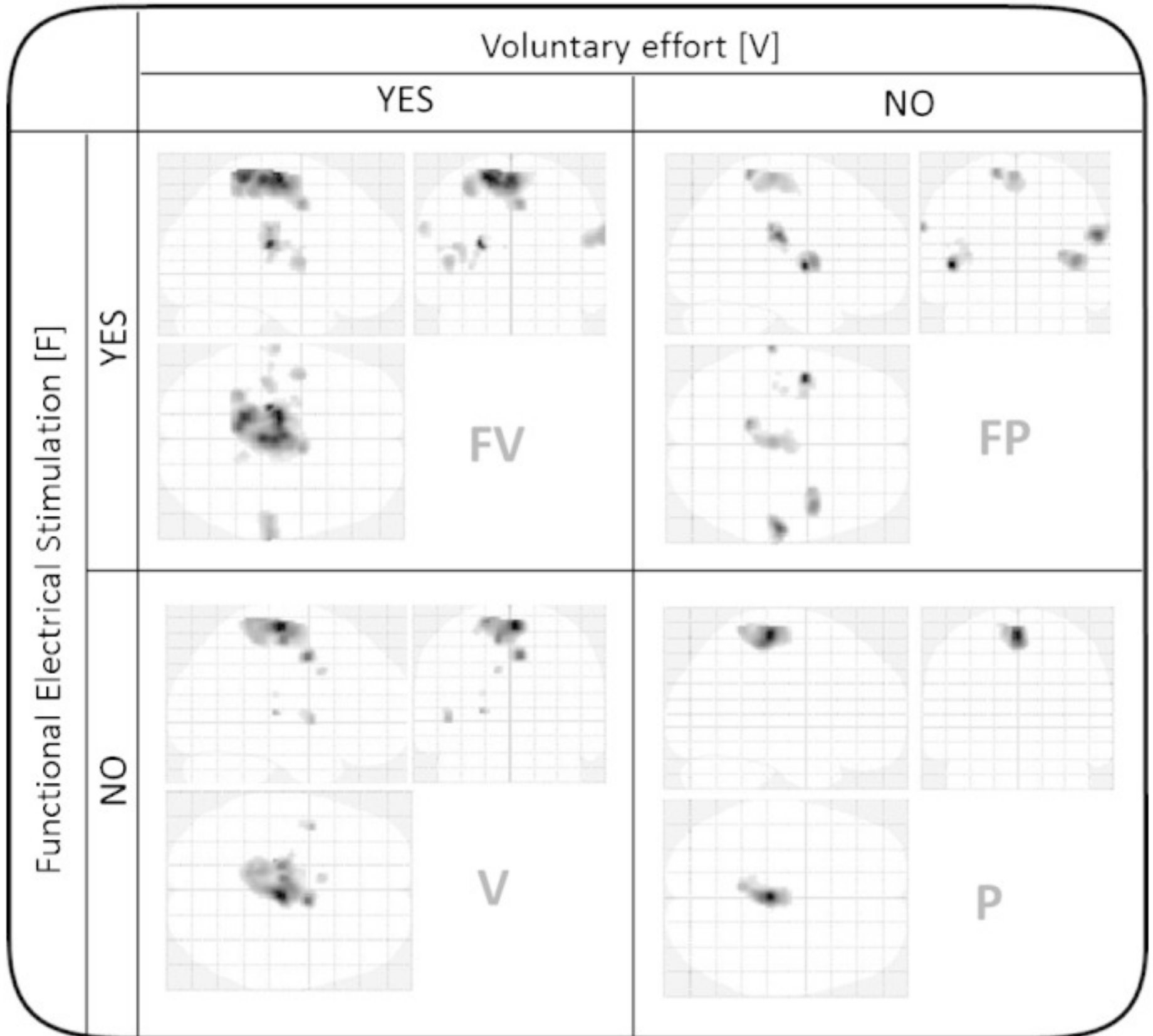
Activation maps for the experimental conditions. Statistical parametric maps (thresholded at p < 0.001, uncorrected for display purposes) showing regions activated in the four conditions using a maximum intensity projection format. FV = FES and voluntary effort; FP = FES induced movement; V = voluntary movement; P = passive movement.

Fig. 3
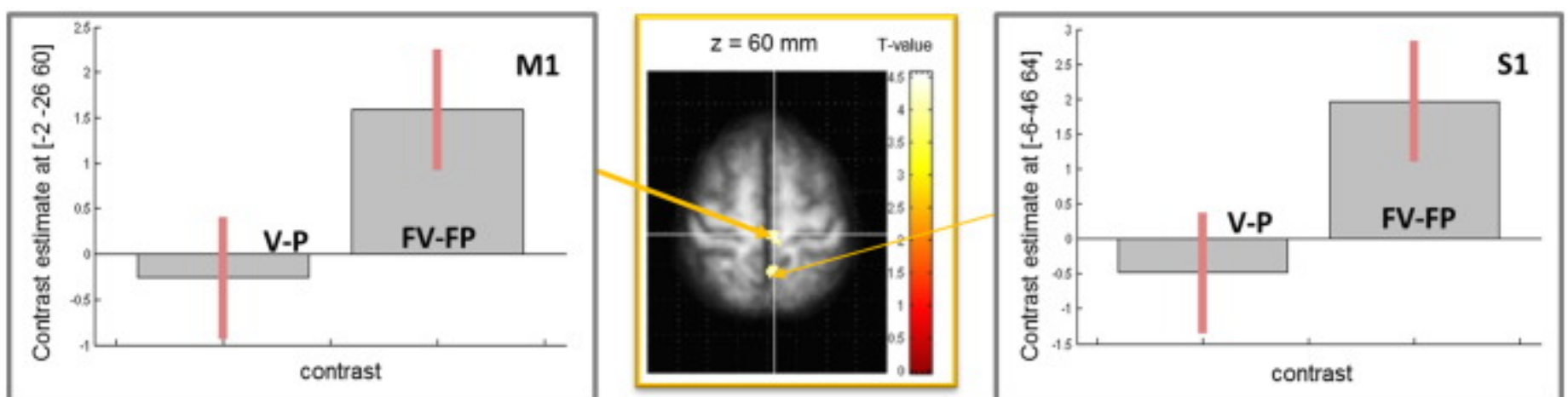
Interaction contrast illustration. Statistical parametric maps (thresholded at p < 0.001, uncorrected for display purposes) showing regions activated for the positive interaction contrast (i.e. (FV − V) − (FP − P)). The slice at z = 60 mm has been chosen for display purpose only. The two plots depict the differences of FV and FP effects, under the regression model;

and the difference between V and P effects for the peak voxel of each cluster (i.e. [− 2, − 26, 60] for M1 and [− 6 − 46 64] for S1). The two clusters are located anatomically in M1 (anterior cluster) and S1 (posterior cluster) leg areas. Red bars represent inter-subject variability (standard error).

Fig. 4
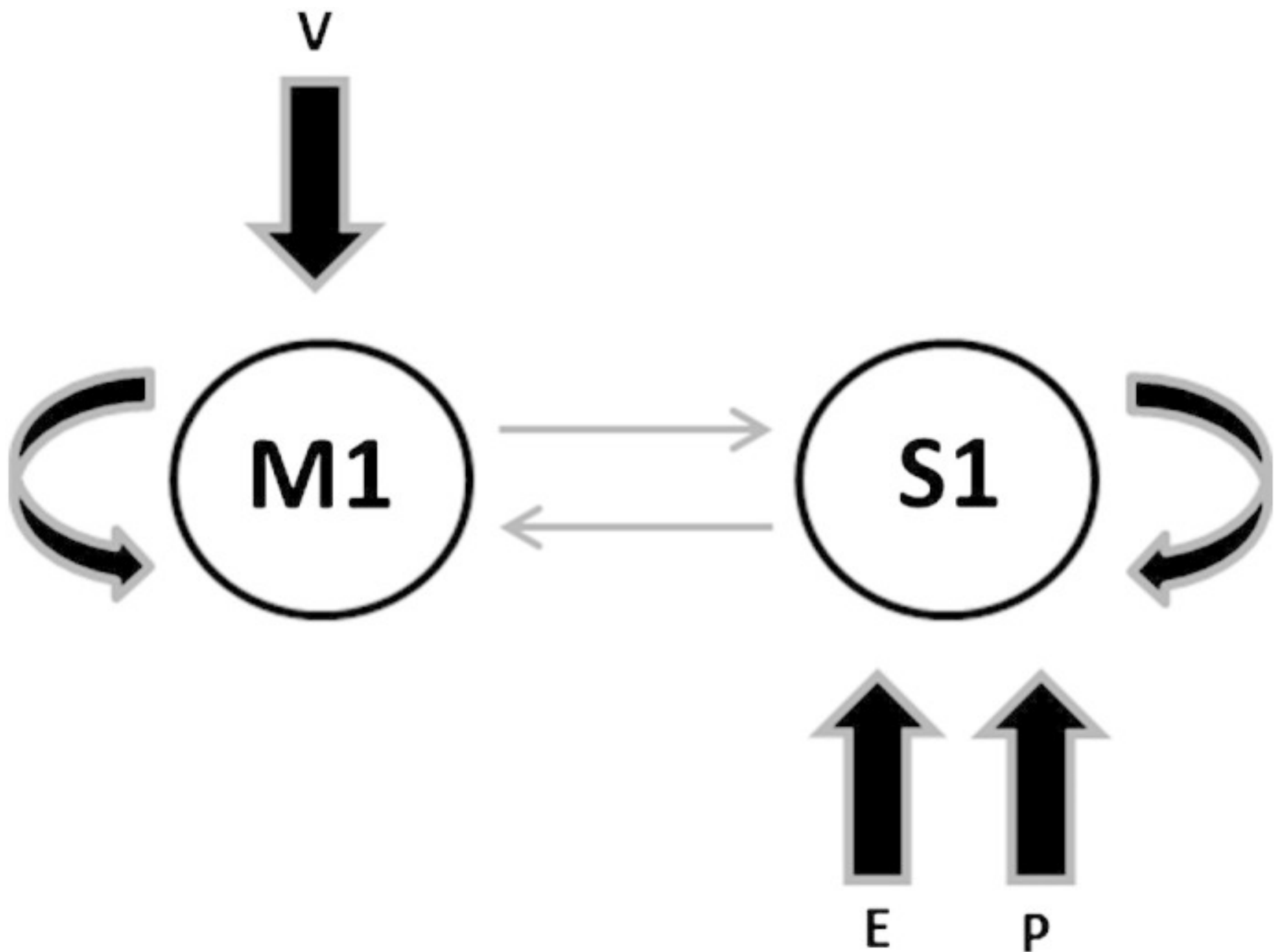
Base DCM. Base two-area DCM with reciprocal connections between the regions (M1, S1). V (effect of voluntary — FV and V onsets) was assumed to drive the system from M1. P (proprioception — all onsets) conveyed information to S1. E (effect of FES — FV and FP onsets) drove S1 as well.

Fig. 5
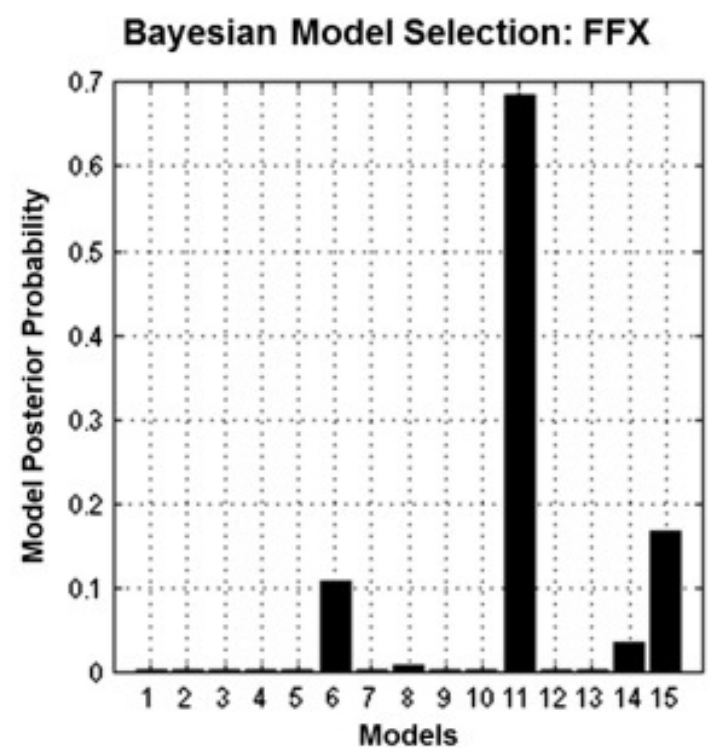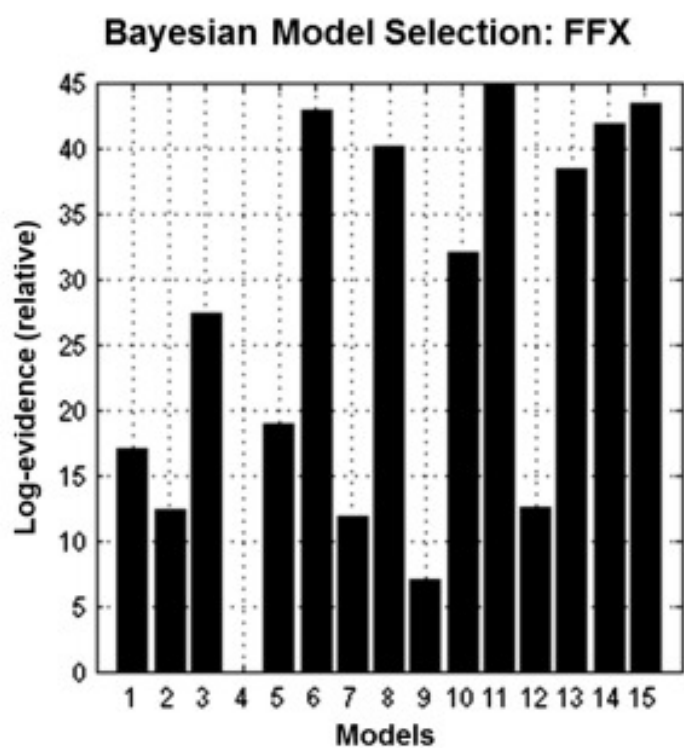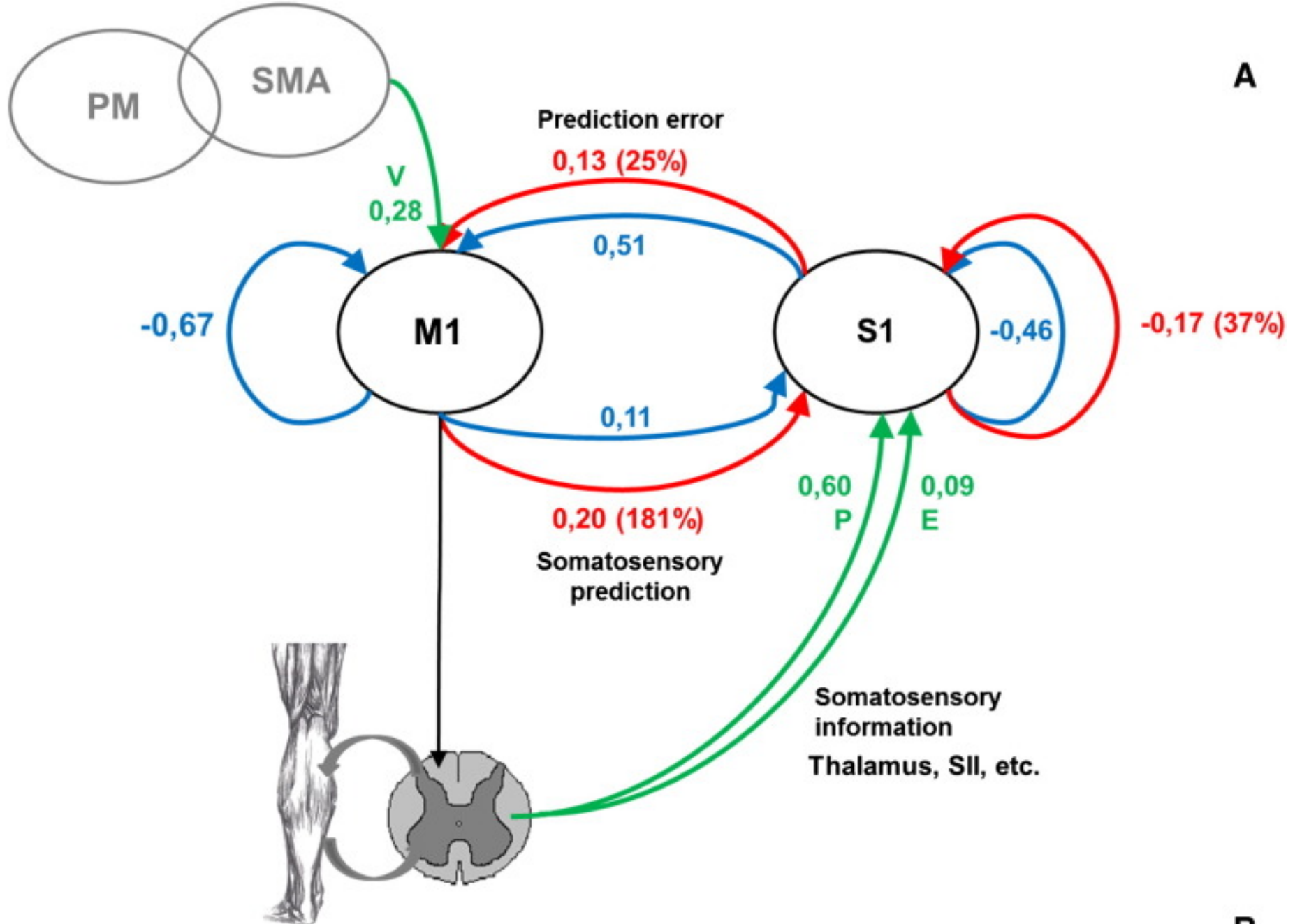
A) Winning DCM among the 15 competing models; B) profile of log evidence (over the 15 models) and the ensuing posterior probabilities.

Table 1

Brain regions active during V, FV, P and FP conditions compared to rest. (+) significant activation at FWE corrected $p < 0.05$ at the whole brain level; (*) significant activation at FWE corrected $p < 0.05$ within predefined ROIs; otherwise reported at uncorrected $p < 0.001$. c = contralateral side; i = ipsilateral side.

MNI coordinates	T	Side	Region

	x	y	z			
V > Rest	− 8	− 16	58	7.55 (+)	c	SMA
	− 16	− 18	68	7.27 (+)	c	SMC (paracentral lobule)
	4	− 20	64	7.19 (+)	i	SMA
	0	− 22	64	6.62 (*)	c	M1 (precentral gyrus)
	− 12	− 42	66	5.80 (*)	c	S1 (postcentral gyrus)
	8	− 2	44	6.64	i	Median cingulate gyrus
	− 44	2	2	5.34	c	Insula
	− 20	− 22	6	4.85	c	Thalamus
	− 18	− 24	20	4.56	c	Caudate nucleus
	− 28	− 6	6	4.12	c	Putamen
FV > Rest	− 14	− 16	64	9.51 (+)	c	SMC (paracentral lobule)
	0	− 26	64	8.09 (+) (*)	c	M1 (precentral gyrus)
	− 8	− 44	68	4.85 (+) (*)	c	S1 (postcentral gyrus)
	− 40	− 24	18	5.52	c	Rolandic operculum
	68	− 22	30	6.36 (*)	i	SII
	− 62	− 18	32	5.47 (*)	c	SII
	− 44	− 2	8	4.9	c	Insula
	− 24	− 2	14	4.57	c	Putamen
	12	− 42	64	4.37	i	Precuneus
	− 50	− 20	16	4.06 (*)	c	PR
	56	− 20	22	5.41 (*)	i	PR
FP > Rest	58	− 18	24	7.59 (+) (*)	i	SII/PR
	− 46	− 2	4	6.79	c	Insula
	− 14	− 42	70	6.04	c	Precuneus
	0	− 26	66	5.44 (*)	c	M1 (precentral gyrus)
	− 12	− 42	66	5.65 (*)	c	S1 (postcentral gyrus)
	− 66	− 26	30	5.95 (*)	c	SII
	42	4	6	5.78	i	Insula
	− 38	− 16	16	4.69	c	Rolandic operculum
	− 50	− 20	18	3.93 (*)	c	PR
P > Rest	0	− 26	62	6.65 (*)	c	M1 (precentral gyrus)
	− 4	− 38	60	5.07 (*)	c	S1 (postcentral gyrus)
	− 6	− 44	66	5.05	c	Precuneus
	54	− 24	26	3.95 (*)	i	SII

Table 2

Brain regions in which there is a significant effect of condition and interaction between conditions. Results reported from ROIs only, at $p < 0.05$ FWE corrected for multiple comparisons within ROIs.

c = contralateral side; i = ipsilateral side.

	MNI coordinates			T	Side	Region
	x	y	z			
FV > V	− 64	− 20	28	3.78	c	SII
	66	− 20	26	5.12	i	SII
	− 60	− 18	24	4.66	c	PR
	62	− 16	24	4.11	i	PR
FP > P	− 66	− 26	34	5.26	c	SII
	− 62	− 14	24	6.71	c	PR
	46	− 8	24	4.41	i	PR
P > FP	0	− 46	56	3.86	c	S1
FV > FP	− 8	− 30	62	5.06	c	M1
	− 6	− 46	60	3.76	c	S1
Main effect Voluntary (V + FV) − (P + FP)	− 12	− 26	66	4.41	c	M1
Main effect FES (FV + FP) − (V + P)	− 64	− 18	24	6.59	c	SII
	60	− 18	28	4.07	i	SII
	− 62	− 16	24	6.71	c	PR
	58	− 18	26	3.86	i	PR
Interaction (FV − V) − (FP − P)	− 2	− 26	60	4.06	c	M1
	− 6	− 46	64	4.18	c	S1